BIOCHEMISTRY
including biophysical chemistry & molecular biology

Article

pubs.acs.org/biochemistry

Measuring Propargyl-Linked Drug Populations Inside Bacterial Cells, and Their Interaction with a Dihydrofolate Reductase Target, by Raman Microscopy

Hossein Heidari-Torkabadi,[†] Tao Che,[‡] Michael N. Lombardo,[§] Dennis L. Wright,[§] Amy C. Anderson,[§] and Paul R. Carey*[,†,‡]

[†]Departments of Chemistry and [‡]Biochemistry Case Western Reserve University, Cleveland, Ohio 44106, United States
[§]Department of Pharmaceutical Sciences, University of Connecticut, Storrs, Connecticut 06269, United States

Supporting Information

ABSTRACT: We report the first Raman spectroscopic study of propargyl-linked dihydrofolate reductase (DHFR) inhibitors being taken up by wild type *Escherichia coli*, *Klebsiella pneumoniae*, and *Staphylococcus aureus* cells. A novel protocol is developed where cells are exposed to the fermentation medium containing a known amount of an inhibitor. At a chosen time point, the cells are centrifuged and washed to remove the extracellular compound, then frozen and freeze–dried. Raman difference spectra of the freeze–dried cells (cells exposed to the drug minus cells alone) provide spectra of the compounds inside the cells, where peak intensities allow us to quantify the number of inhibitors within each cell. A time course for the propargyl-linked DHFR inhibitor UCP 1038 soaking into *E. coli* cells showed that penetration occurs very quickly and reaches a plateau after 10 min exposure to the inhibitor. After 10 min drug exposure, the populations of two inhibitors, UCP 1038 and UCP 1089, were ~1.5 × 10^6 molecules in each *E. coli* cell, ~4.7 × 10^5 molecules in each *K. pneumonia* cell, and ~2.7 × 10^6 in each *S. aureus* cell. This is the first in situ comparison of inhibitor population in Gram-negative and Gram-positive bacterial cells. The positions of the Raman peaks also reveal the protonation of diaminopyrimidine ring upon binding to DHFR inside cells. The spectroscopic signature of protonation was characterized by binding an inhibitor to a single crystal of DHFR.

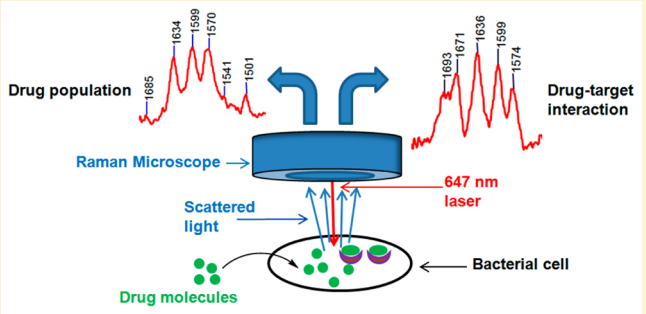

The ability to monitor the populations and reactions of drug-like molecules with their target enzymes inside bacterial cells is critical for antibiotic drug development. A major challenge in this field is to develop a technique which enables us to readily quantify populations of a drug molecule inside bacterial cells. Such information may provide insight into why compounds with good *in vitro* activity have poor biological properties. Moreover, for a series of molecules such studies will create "league tables" that can provide insight into the chemical factors that promote cell penetration and subsequent compound retention.[1−6]

Raman spectroscopy is a light scattering technique which utilizes the interaction of light with molecules to measure vibrational properties of molecules. When light interacts with molecules, some photons are scattered, and while most of the scattered photons from a sample have same frequency as the incident light, a small fraction of photons scatter at different frequencies due to the exchange of the energy between the photons and vibrational energy levels of the sample molecules. Thus, by measuring the change in energy of the photons, the vibrational properties of the scattering molecules can be obtained. In turn, the vibrational spectrum informs on molecular structure and interactions.[7−10]

Raman spectroscopy has been used for studying various biological systems including proteins, nucleic acids, lipids, and carbohydrates as well as the characterization of bacterial and mammalian cells.[11,12] Previous studies also exploit Raman spectroscopy as an imaging technique to locate lipids, nucleic acids, and drug molecules in mammalian cells.[13−18] In addition, Raman spectroscopy is a powerful technique in studying reactions and structural changes in enzyme and drug complexes.[19,20] In the present context, advantages of the Raman approach include characteristic Raman signatures for each drug molecule, short times (minutes) for data collection, and the fact that the technique is label free and nondestructive.

Using Raman spectroscopy, we are able to provide information on both populations and structural changes in drug molecules within cells. The former derives from the fact that Raman intensities of characteristic drug peaks are directly proportional to the population. In addition, by monitoring the position of the peaks in the Raman spectrum derived from the

Received: February 26, 2015
Revised: April 13, 2015
Published: April 14, 2015

DOI: 10.1021/acs.biochem.5b00202
Biochemistry 2015, 54, 2719−2726

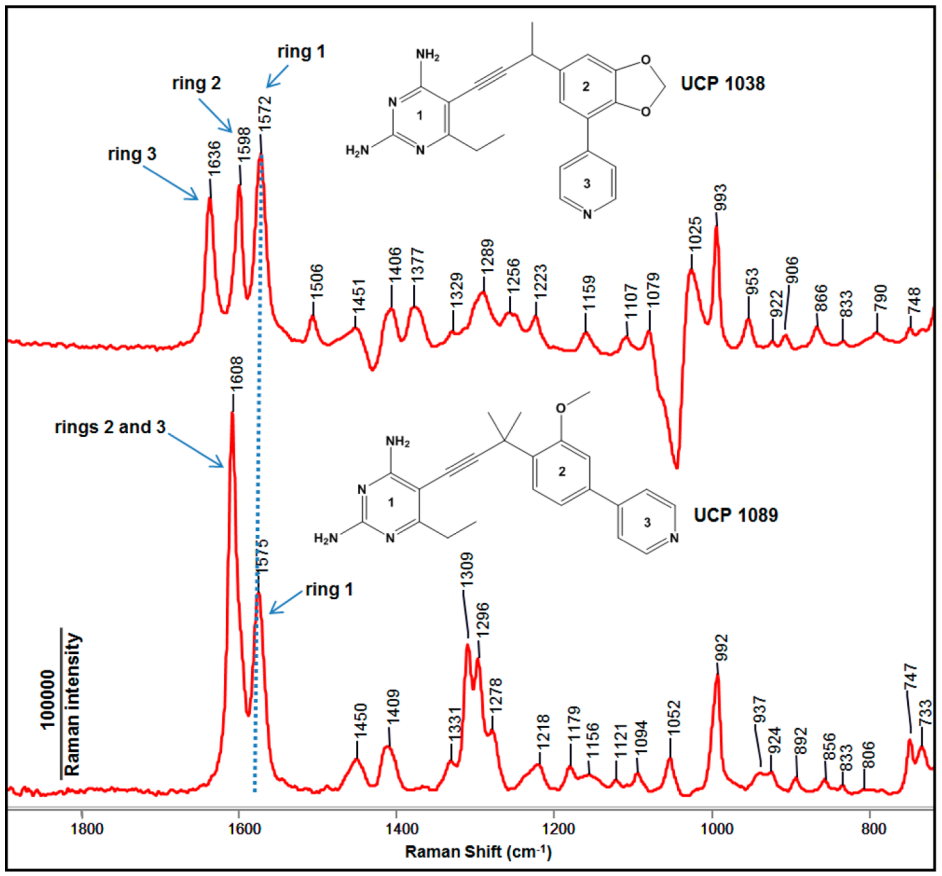

Figure 1. Raman spectra of UCP 1038 (top) and UCP 1089 (bottom) with their chemical structures. The peaks around 1572 cm^{-1} in both spectra are assigned to a diaminopyrimidine ring (ring 1) mode in both compounds. (Both compound were dissolved in DMSO separately, with the final concentration of 50 mM. The spectrum of DMSO was subtracted from each spectrum. The negative peak around 1050 cm^{-1} in the top spectrum is caused by subtraction of DMSO, since we did not have perfect overlap in this case.).

drug molecules, we are able to detect their reactions and (quasi)stable intermediates inside cells.[21]

Recently, we reported a protocol, where cells are grown in the presence of the drug, which enabled us to identify clavulanic acid and tazobacatam intermediates inside *E. coli* cells. Moreover, we could quantify the number of these β-lactamase inhibitors inside the cells.[21] The method relies on Raman difference spectroscopy, the cells are frozen and freeze−dried and the difference spectrum (cells that were exposed to drug minus cells alone) provides the Raman spectrum of the intracellular drug molecules. Here, we report a modified protocol which enables us to follow the kinetics of propargyl-linked dihydrofolate reductase inhibitor uptake in *Escherichia coli*, *Klebsiella pneumoniae*, and *Staphylococcus aureus* cells using Raman intensity of the compound's diaminopyrimidine ring mode. In addition, the shift in the diaminopyrimidine ring mode demonstrates the protonation of N-1 in diaminopyrimidine ring upon binding to DHFR enzyme inside *E. coli*. This is the first time we have obtained result from a Gram-positive bacteria for direct comparison with Gram-negative cells.

The recent protocol has some advantages compared to the former one; the new protocol involves soaking the drug into cells after they have reached their growth plateau. Soaking for different time points allows us to monitor the kinetics of drug diffusion into the cell, and the formation of drug−target intermediates on the time scale of minutes. Additionally, by using the new protocol, we can avoid many of metabolic changes that occur inside cells when the cells are actively growing in the presence of drug. As a result, the Raman difference spectra from this approach are easier to interpret and we have a clearer view of unreacted drug inside the cells, or drug−target complexes, without interference from peaks generated by metabolic changes.

MATERIALS AND METHODS

Bacterial Strains and Genetic Constructs. *Escherichia coli* BW25113,[22] *Klebsiella pneumoniae*, and *Staphylococcus aureus* (ATTC 43300) were used to measure the populations of UCP 1038 and UCP 1089 (see Figure 1 for structures) inside these wild type cell lines. For the experiment requiring a large intracellular population of DHFR, the *E. coli* DHFR gene was cloned into a pET-41(a)+ plasmid vector. *E. coli* BL21 (DE3) cells (Stratagene, La Jolla, CA), as the host strain, was transformed by the vector, and exploited for overexpression of DHFR protein.

Raman Spectroscopy of Bacterial Cells. In this protocol, we used *E. coli*, *K. pneumoniae*, or *S. aureus* cells. Cells were grown at 37 °C with agitation in Mueller Hinton broth (Difco) to an OD_{600} of 0.8. For each time point, 10 mL of 0.8 OD_{600} culture of cells were distributed in a tube. The cells were pelleted and washed with buffer (dibasic potassium phosphate 0.067 M and magnesium chloride 0.01 M, pH 7.3). In the next step, 100 μg of UCP 1038 or UCP 1089 dissolved in 1 mL of culture medium was used to resuspend the cell pellet. Cells were centrifuged in 3500 rpm and washed with the buffer after 1, 10, 30, or 60 min in suspension. They were frozen and

DOI: 10.1021/acs.biochem.5b00202
Biochemistry 2015, 54, 2719−2726

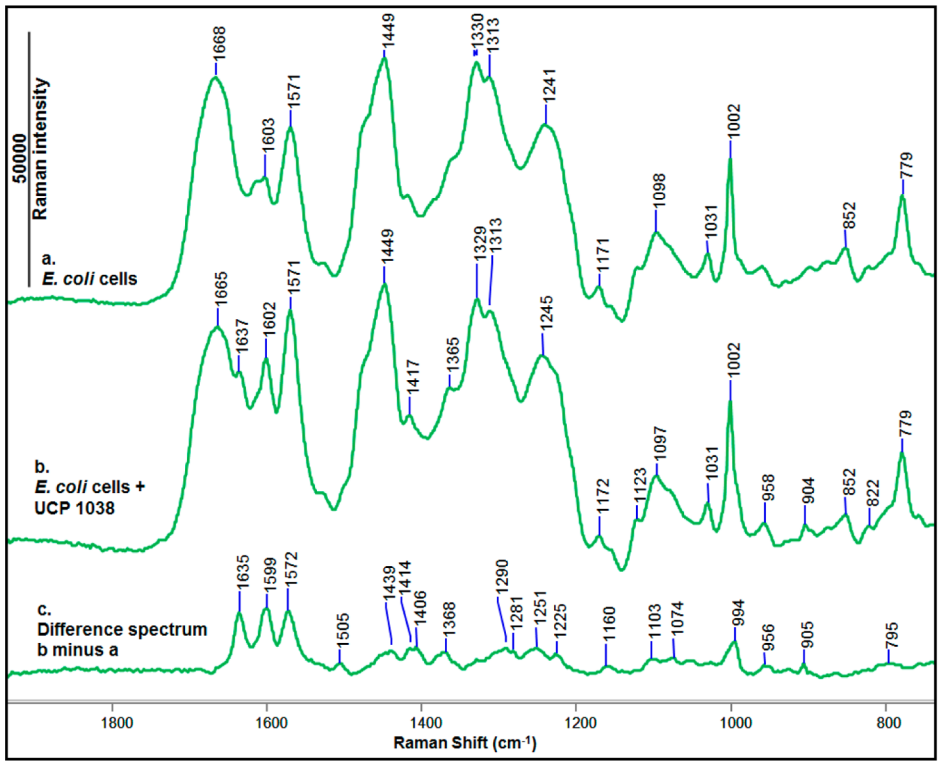

Figure 2. Raman spectra: (a) freeze−dried *E. coli* cells, (b) freeze−dried *E. coli* cells with 25 μg UCP 1038, (c) Raman difference spectrum, b minus a.

freeze−dried immediately after washing. Raman spectra were taken from each sample. The spectra were obtained from lyophilized powder on an aluminum foil mounted on the Raman microscope stage.[19] Data collection and processing were performed using HoloGRAMS and GRAMS/AI7 software (ThermoGalactic, Salem, NH). Raman difference spectra were obtained using [(cells treated with drug) minus (cells without drug)]. In a control experiment to verify that the same number of cells are present in both samples (with and without drug) and the features in difference spectra are related to drug, the procedure was repeated where both samples did not contain drug. The difference spectrum contained no observable Raman features.

The discussion of Raman spectra presently focuses on the "double bond spectral region" 1500 to 1700 cm^{-1}. This facilitates the quantification of the compounds' populations since it contains the most intense peaks. Moreover, major changes occur in the position of the ring mode from the ring one upon protonation of the N-1 atom allowing us to follow this event.

Cloning and Expression of DHFR in *E. coli* Cells. Recombinant DHFR enzyme was overexpressed in *E. coli* BL21(DE3) cells in Luria−Bertani Broth containing 30 ug/mL kanamycin at 37 °C, through induction with 1 mM IPTG followed by an additional 3 h incubation period at 37 °C. For each sample, 5 mL of the culture was pelleted and washed thoroughly with washing buffer and used to monitor protonated UCP 1038 inside *E. coli* cells.

Crystallization of *S. aureus* DHFR. Procedures for cloning and purification of *S. aureus* DHFR have been reported previously.[23] *S. aureus* DHFR was crystallized via the hanging drop method using recombinant protein with the concentration of 16 mg/mL. Crystallization conditions consisted of 15% PEG 10 000, 150 mM sodium acetate, 100 mM MES pH 6.5, and 5% γ-butyrlactone.[23] Crystals were formed within 3−5 days at 4 °C.

Raman Crystallography. The Raman microscopy technique for single crystals has been described previously.[19,20] A *S. aureus* DHFR crystal was transferred into a solution containing 0.1 M MES, 0.1 M sodium acetate, and 13% PEG 10 000 at pH 6 on a siliconized glass coverslip and transferred into a hanging drop setup in a crystallization tray. A 80 mW 647 nm Kr^+ laser beam (Innova 70 C, Coherent, Palo Alto, CA) was focused into the protein crystal via the microscope using a 20× objective. The Raman spectrum of an apo crystal was acquired for 100 × 1 s accumulations. Then 0.5 μL of 20 mg/mL UCP 1038 or UCP 1089 in DMSO was added to the 4.5 μL hanging drop around the crystal. Raman spectra of the reaction of the *S. aureus* DHFR crystal with UCP 1038 or UCP 1089 were acquired for 100 × 1 s accumulations and were averaged for each time point serially every 2−3 min. For each condition, one spectrum from the buffer around the crystal was also recorded and subtracted from the crystal spectrum. To acquire the Raman difference spectrum for each time point, the Raman spectrum of the *S. aureus* DHFR apo crystal was subtracted from the Raman spectrum of the crystal plus compound at each time point. For the soak-out experiment, after the crystal stayed 60 min in a drop containing UCP 1038, the buffer around the crystal was exchanged by fresh buffer without UCP 1038 for few times, and then the spectra was recorded from the crystal every 5 min. The soak-out condition is used to remove nonspecifically bound compounds (compounds which are not bound to the active site and are usually bound more weakly) from the crystal.

Quantum Mechanical Calculation. To help peak assignment in the Raman spectra of UCP 1038 and UCP 1089, *ab*

DOI: 10.1021/acs.biochem.5b00202
Biochemistry 2015, 54, 2719−2726

initio quantum mechanical calculations were preformed on the Case Western Reserve University's cluster facility. Calculations were performed at the density functional theory level using the 6-31+G(d) basis set. Density functional theory calculations were performed with Becke's three parameters hybrid method using the correlation functional of Lee, Yang, and Parr (B3LYP).[24,25] *GaussView* software was used to reveal which molecular vibrations contribute to the peaks.

RESULTS

Raman Intensity Reference Curve. Initially a reference curve is constructed to correlate the Raman intensity of a marker band from the unreacted ligand to the known amount of the ligand mixed with a known amount of cells. For UCP 1038 and UCP 1089 quantum mechanical (Gaussian) calculations show that the intense peak near 1572 cm^{-1} (Figure 1) is an isolated ring vibration for the diaminopyrimidine group, ring 1 (confirming earlier Raman studies[26]), and it is used as a marker where, as a working approximation, its intensity is directly proportional to the amount of compound in the sample. In DMSO solutions at exactly 50 mM, the 1572 cm^{-1} band for UCP 1038 and UCP1089 had the same absolute intensity to ±2%. To generate the reference curve 10 mL aliquots of 0.8 OD_{600} (~10^9 cfu/mL) culture of cells are pelleted. The pellets are washed with buffer and resuspended in 250 μL of the same buffer containing 1, 2.5, 5, 10, 25, or 50 μg of UCP1038. A control pellet is resuspended in 250 μL buffer alone. The mixtures are frozen immediately by immersing the tubes in liquid nitrogen. The frozen mixtures are freeze−dried, and the Raman spectra are recorded from each powdered sample under the Raman microscope. After Raman difference spectra are obtained [(cells with drug) minus (cells without drug)] (Figure 2), the intensity of the 1572 cm^{-1} marker band (from ring one, Figure 1) is measured and ratioed to the 1449 cm^{-1} peak (an internal standard from CH_2 vibrations from all molecules in the cells containing $-CH_2$ groups[27]) from each original spectrum (cells plus drug, see Figure 2). Peak intensities are measured by peak heights at 1449 cm^{-1} above the estimated background between 1420 and 1500 cm^{-1}. Figure 3 shows the ratio, which is plotted against the amount of compound in each sample. It has been assumed that the intensity of the diaminopyrimidine ring mode near 1572 cm^{-1} is constant under all experimental conditions (from the neutral form of the diaminopyrimidine ring). The data shown in Figure 3 are from three experiments, and the error bars indicate good reproducibility.

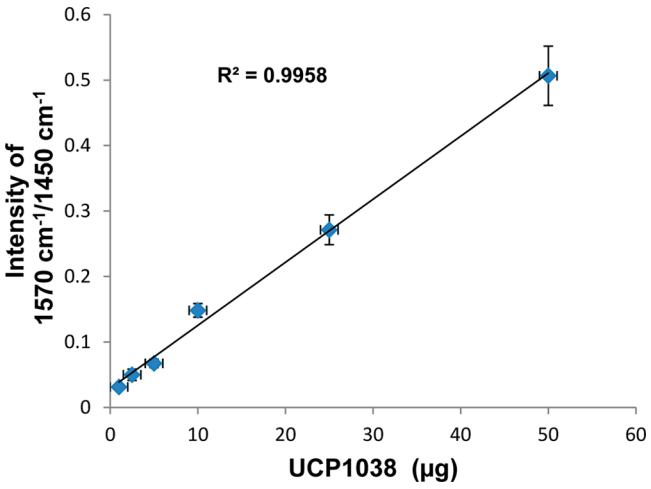

Figure 3. Calibration curve: quantity of UCP 1038 compound added to cells vs relative intensity of 1038 ring 1 band.

Measuring the Populations of UCP 1038 and UCP 1089 in *E. coli*, *K. pneumoniae*, and *S. aureus*. To measure the amount of compound inside the cells, using the most recent protocol, cells are grown to 0.8 OD_{600} and harvested from 10 mL of culture by centrifugation. The cell pellet is washed with buffer, and resuspended in 1 mL of culture medium containing a 100 μg of UCP 1038 or UCP 1089. After different incubation periods (1, 10, 30, or 60 min), each mixture is centrifuged, and most drug outside the cells is removed when the medium is discarded. The pellet is washed thoroughly with buffer to remove the residual compound from outside the cells, then frozen, and then freeze−dried. The Raman spectrum is recorded from freeze−dried cells, and after obtaining Raman difference spectrum (cells with drug minus cells alone), the intensity of 1572 cm^{-1} marker is ratioed to 1449 cm^{-1} from the original spectrum (Figure 2). By plotting this ratio on the reference curve (Figure 3) the amount of UCP 1038 or UCP 1089 present in the cell pellet was calculated. To estimate the number of compound molecules present inside each cell, first the number of cells present in the 0.8 OD_{600} culture is estimated by serial dilution of the culture, followed by counting the number of colony formations on agar plates (cfu/mL). By knowing the amount of UCP 1038 or UCP 1089 and the number of cells present in the sample, the amount of compound inside each cell can be calculated (see ref 15 and Supporting Information therein).

The Raman signal comes from a number of cells located in the focal volume of the laser. To test the assumption that the calibration curve can be used for all three cell lines, we assume that we have a similar number of cells in the focal volume, according to the size similarity among the three cell lines and by measuring the absolute Raman intensities for each cell line we see less than ±5% variations.

A simple time course for UCP 1038 population build up in *E. coli* is listed in Table 1, and provides two immediate insights.

Table 1. Quantifying the Number of UCP 1038 Molecules Inside each WT *E. coli* after 1, 10, and 60 Min Drug Exposure[a]

	UCP1038	
time of exposure	I 1573 cm^{-1}/I 1450 cm^{-1}	number of UCP 1038 molecules per each *E. coli* cell
1 min	0.210	8.56×10^5
10 min	0.322	1.38×10^6
60 min	0.356	1.55×10^6

[a]For each time point there is a 3 to 5 min lag time for centrifugation and washing the cell pellet before freezing the sample. The numbers are the average for more than three experiments and are reproducible to within ±6%.

The drug penetrates the cells quickly and there is a major intracellular population at 1 min drug exposure, and second, the population of the drug increases until 10 min soaking but then remains approximately constant until 60 min.

Figures 4 and 5 show Raman difference spectra of UCP 1038 and UCP 1089 inside *E. coli*, *K. pneumoniae*, and *S. aureus*, respectively, after 10 min drug exposure. The ratio of the band around 1572 cm^{-1} to the 1449 cm^{-1} internal standard (Figure

DOI: 10.1021/acs.biochem.5b00202
Biochemistry 2015, 54, 2719−2726

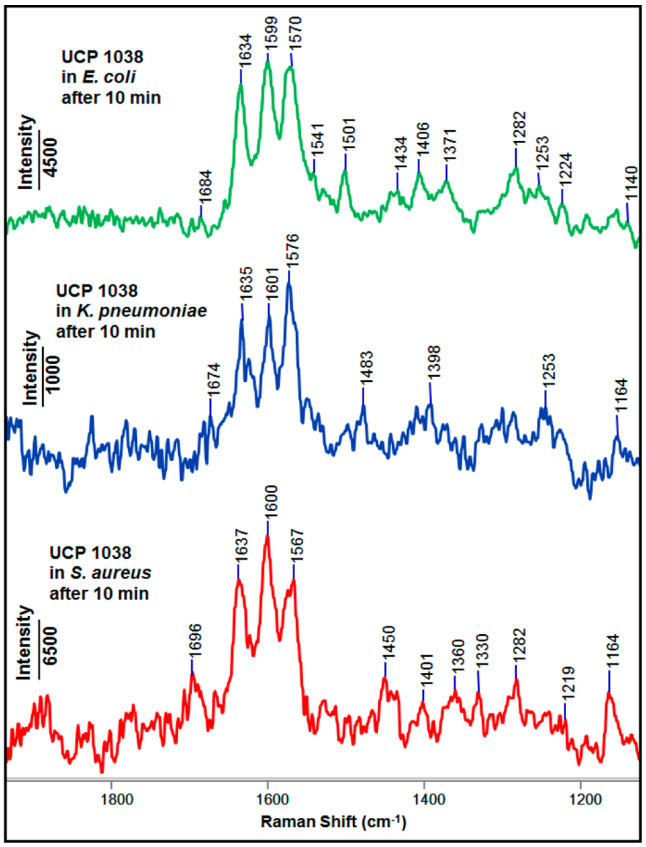

Figure 4. Raman difference spectra of *E. coli* (top), *K. pneumoniae* (middle), and *S. aureus* (bottom) cells after 10 min exposure to the UCP 1038.

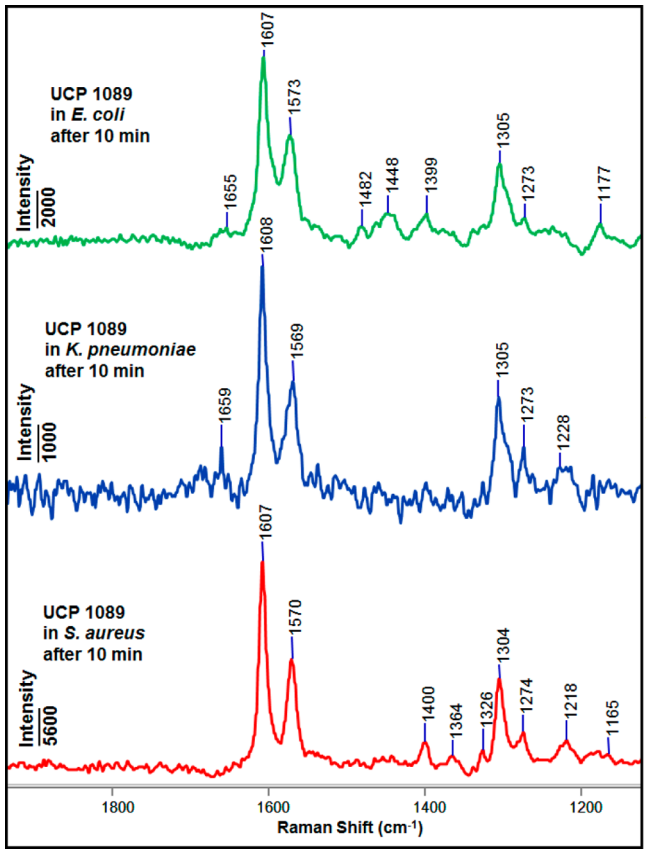

Figure 5. Raman difference spectra of *E. coli* (top), and *K. pneumoniae* (middle), and *S. aureus* (bottom) cells after 10 min exposure to the UCP 1089.

3) for UCP 1038 is 0.321 for *E. coli*, 0.117 for *K. pneumoniae*, and 0.466 for *S. aureus*. For UCP 1089 the values are 0.368 for *E. coli*, 0.141 for *K. pneumoniae*, and 0.806 for *S. aureus*. Using a standard curve, derived as described above, the number of molecules per cell after 10 min of drug exposure was calculated and these values are listed in Table 2.

Raman studies of UCP 1038 and UCP 1089 Bound to DHFR Crystals Shows Protonation of Nitrogen (N-1) in the Diaminopyrimidine Ring. To study the Raman spectrum of UCP 1038 bound to DHFR, the DHFR protein from *Staphylococcus aureus* was crystallized. A single crystal of DHFR was used in a hanging drop containing crystallization solution. A Raman spectrum of apo-DHFR crystal is shown in Figure S1 (see Supporting Information). 0.5 μL of 50 mM (20 mg/mL) UCP 1038 in DMSO was added yielding a final concentration of 5 mM. This soaked into the single crystal to provide the bound UCP 1038 species.

Figure 6 shows the Raman spectrum of unbound UCP 1038 (top) and Raman difference spectra of a DHFR crystal with UCP 1038 after 20 and 60 min. At 20 min, we see a 1665 cm^{-1} feature in the spectrum rather than 1572 cm^{-1} peak from the original UCP 1038 spectrum. This is explained by protonation of N-1 of the diaminopyrimidine ring which is a universal feature in all crystallographic studies of DHFR complexes, for example in *Candida glabrata* DHFR crystal.[28]

As we increase the soaking time, extra UCP 1038 binds within the crystal nonspecifically (i.e., not in the active site), which could be seen in the 60 min spectrum (1573 cm^{-1} peak and increase in the intensity of 1604 and 1637 cm^{-1} peaks). These extra nonspecifically bound species (neutral form) could

Table 2. Quantifying the Number of UCP 1038 and UCP 1089 Molecules Inside Each WT *E. coli*, *K. pneumoniae*, and *S. aureus* Cell after 10 Min Drug Exposure[a]

compound	number of molecules in each *E. coli* BW25113 cell	number of molecules in each *K. pneumoniae* cell	number of molecules in each *S. aureus* ATCC 43300 cell
UCP 1038	1.38×10^6	4.1×10^5	2.0×10^6
UCP 1089	1.60×10^6	5.3×10^5	3.45×10^6

[a].The numbers are the average for three experiments and are reproducible to within ±4−6%.

be removed by exchanging the holding buffer around the crystal with a fresh buffer without UCP 1038. This can be seen in the bottom spectrum in Figure 6 where the protonated UCP 1038 band near 1665 cm^{-1} remains after the soak out, although the 1573 cm^{-1} band disappears. To confirm that the band near 1670 cm^{-1} is due to protonated diaminopyrimidine ring, we carried out a Gaussian quantum mechanical calculation. For the simple compound derived from UCP 1038 (Figure 1) by replacing rings 2 and 3 by a methyl group, the calculation showed that upon protonation at N-1 the breathing mode for ring 1 shifted to 1645 cm^{-1} compared to 1572 cm^{-1} for the neutral ring.

In a similar set of experiments, UCP 1089 was soaked into *S. aureus* DHFR single crystal. Figure S2 (Supporting Information) shows the Raman difference spectrum of UCP 1089 soaked into the single crystal after 30 min. A peak at 1665 cm^{-1}

DOI: 10.1021/acs.biochem.5b00202
Biochemistry 2015, 54, 2719−2726

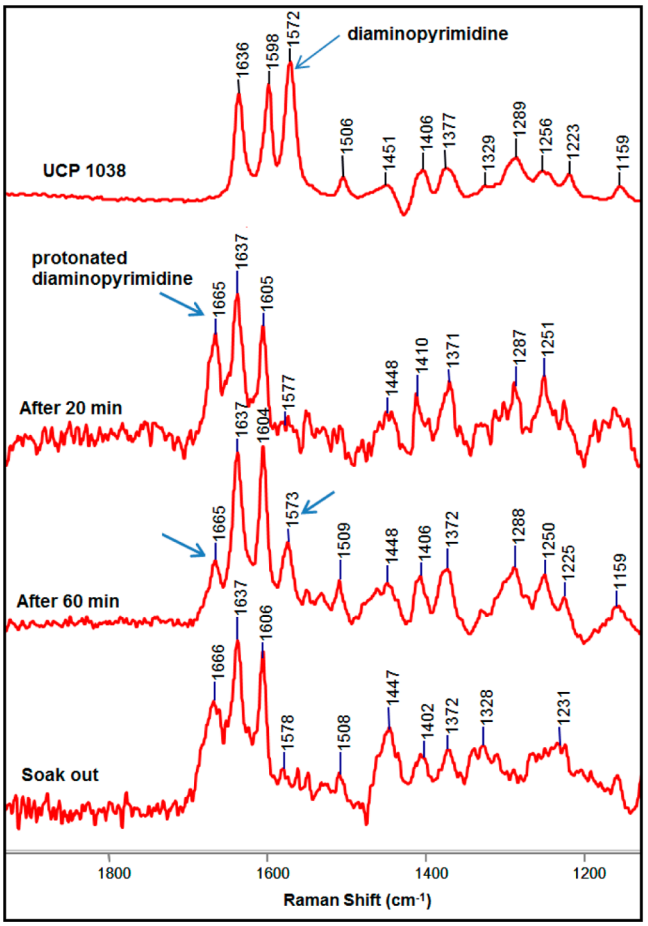

Figure 6. Raman spectrum of UCP 1038 (top) and Raman difference spectra of DHFR crystal with UCP 1038 after 20 and 60 min infusion, and soak-out experiment. For the soak-out spectrum, the holding buffer around the DHFR crystal after 60 min was exchanged with a fresh buffer without UCP 1038.

is assigned to the protonated N-1 in diaminopyrimidine ring of UCP 1089.

Although the DHFR enzyme in this experiment was from *S. aureus* and was used based on the crystal's ready availability (from the Anderson lab), the key residues responsible for ligand binding in the active site share 100% identity with *E. coli* DHFR.

Monitoring Protonated UCP 1038 and UCP 1089 upon Binding DHFR Protein Inside *E. coli* Cells. To study the protonated (bound) forms of UCP 1038 or UCP 1089 inside cells, we exploited *E. coli* cells containing plasmid to overexpress the DHFR protein (see Materials and Methods). The reason that we only observed free or unbound UCP 1038 and UCP 1089 inside wild type *E. coli* or *K. pneumoniae* is that the number of DHFR molecules in these cells are estimated to be a few hundred;[29] thus, the bound UCP 1038 or UCP 1089 is below our detection limit. However, the population of DHFR molecules in the overexpressed cells is about 200-fold more than wild type cells.

In this experiment, 50 μg UCP 1038 or UCP 1089 dissolved in washing buffer was added to a washed pellet from 5 mL of the culture. After 20 min of soaking the mixture was frozen by immersing the tube in liquid nitrogen. The frozen mixture was freeze–dried and used for Raman microscopy. The control sample was prepared in a similar manner without adding the compound into the pellet. We did not centrifuge and wash the cells after soaking in UCP 1038 or UCP 1089 in order to attempt to see both free and DHFR-bound compound in the same experiment. Figure 7 shows the Raman difference spectra

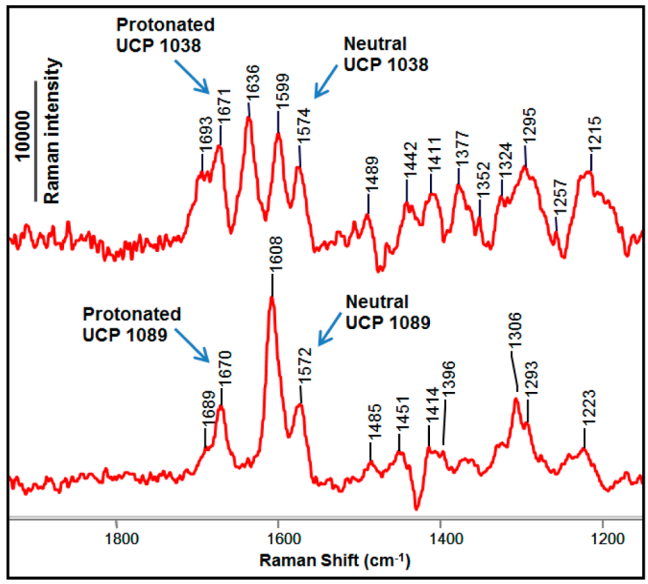

Figure 7. Raman difference spectrum of freeze–dried *E. coli* BL21 (DE3) cells containing overexpressed DHFR protein incubated with UCP 1038 and UCP 1089 for 20 min.

of the freeze–dried mixture which gratifyingly is very similar to the spectra of UCP 1038, or UCP 1089 soak into *S. aureus* crystal (see Figure 6 and Figure S2). Peaks around 1574 cm^{-1} are from free, neutral UCP 1038 or UCP 1089, whereas ~1671 cm^{-1} features in the spectra are assigned to the protonated diaminopyrimidine ring of both compounds bound to DHFR. The increase in the relative intensities of 1599 and 1636 cm^{-1} bands in the top spectrum and 1608 cm^{-1} band in the bottom spectrum (Figure 7) compared to free UCP 1038 and UCP 1089 (Figure 1) is due to the contribution from both neutral and protonated forms of the compounds. The DHFR bound population is inside the cells and the free population is intra- and extracellular. This raises the possibility that quite sophisticated titrations could be undertaken in future experiments. Non inhibitor Raman bands can be seen in Figure 7, e.g., bands near 1215, 1295, and 1693 cm^{-1}. These are likely due to metabolic changes in the cells caused by the DHFR inhibitor binding to its target. This is an ongoing study in our lab.

DISCUSSION

In this study we introduce our new protocol to study drug populations and interactions inside bacterial cells. Our new protocol has the advantage of being able to follow a time course for population of drug molecules inside cells. In addition, this study uses a different class of compounds from our previous study (which involved β-lactam inhibitors) and shows the general application of the method to study various classes of antibacterial compounds. Using compounds that show fairly intense and characteristic Raman features facilitates the detection and quantitation of the compound. Compounds that have regions of π-electron conjugation usually meet this criterion.

DOI: 10.1021/acs.biochem.5b00202
Biochemistry 2015, 54, 2719–2726

The values summarized in Table 2 were obtained from 10 min drug exposure in an effective compound concentration of 10 μg/mL (100 μg compound was added to the pellet from 10 mL of 0.8 OD_{600} culture). Our Raman data for UCP 1038 and UCP 1089 bound in a single crystal of DHFR show that the ring mode for diaminopyrimidine shifts from ~1573 cm^{-1} (neutral form) to ~1665 cm^{-1} upon protonation. Thus, we conclude the Raman difference spectra of UCP 1038 and UCP 1089 in all three wild type cell lines (Figures 4 and 5) are from unbound (neutral form) compounds inside cells. The fact that we have a few hundred molecules of DHFR in each cell, compared to 10^3 times more UCP molecules, strongly supports the conclusion that we observe neutral (unbound) UCP molecules inside the cells. Figure 7 also supports our conclusion, since when we increase the population of DHFR inside the cells, we are able to observe the protonated (bound) form of both compounds inside *E. coli* cells.

Although we are only monitoring unbound compound in all three cell lines, a conclusion can be drawn from the population of UCP 1038 and UCP 1089 inside these cells. The difference between the population of two compounds in a Gram-negative cell line is only ~1.3-fold, whereas the differences between *E. coli* and *K. pneumoniae* for the same compound is 3- to 4-fold, where *E. coli* has the higher population. In *S. aureus*, a Gram-positive bacteria, the population of the two compounds in the same cell line varies by about ~1.7-fold, but the populations of both compound inside *S. aureus* are 5- to 6-fold higher than *K. pneumoniae*, and about 2-fold higher than *E. coli*. The higher population of compounds in *S. aureus* could be explained by lack of outer membrane in Gram-positive compared to Gram-negative bacteria. It is of interest that in our initial publication[21] for 10 μg/mL of clavulanic acid soaking into *E. coli* DH10B (WT) cells yielded 2.2×10^6 clavulanic acid molecules per cell. However, the conditions were different, the growing cells were exposed to clavulanic acid for about 4 to 6 h until the OD reached 0.8, whereas here we are resuspending the cell pellet from 0.8 OD_{600} culture in 1 mL medium containing of DHFR inhibitor (10 μg for cell pellet from each ml) for 10 min. It should be noted under the present condition of inhibitor and cell concentrations, and time of exposure, that we do not see evidence for cell lysis using a light microscope.

The present results coupled with our earlier publication[21] clearly indicate that we can measure drug population within bacterial cells and follow chemical changes involving drug–target interactions and reactions. An important issue is sensitivity. With our present equipment and sample protocols it will be difficult to obtain Raman signal from less than 10^4 drug molecules per cell, even for molecules such as the UCP compounds which have intense (nonresonance) Raman signals. There are several means to improve sensitivity significantly, at the sample preparation level and with optical equipment.

Raman signals are directly proportional to the power of the laser used to excite the spectrum. Although high power leads to sample destruction, this might be overcome by using a variation of the Kiefer and Bernstein spinning cells.[30] Raman microscopes usually do not have high photon throughput. This can be improved by using a directly coupled microscope that features a minimal number of components or dispensing with the microscope and using a classical 90° excitation scattering collection in front of spectrograph.[10] We are confident that an improvement of at least 10× in Raman signals and perhaps as high as 100× can be gained. This will bring our detection limit close to the cell/drug concentrations used to measure MICs and assist us to directly relate changes in drug retention to biological activity.

■ ASSOCIATED CONTENT

Supporting Information

Raman spectrum of apo-DHFR crystal and Raman difference spectrum of UCP 1089 bound to a single crystal of *S. aureus* DHFR. The latter spectrum shows protonation of UCP 1089 upon binding to the enzyme. This material is available free of charge via the Internet at http://pubs.acs.org.

■ AUTHOR INFORMATION

Corresponding Author

*E-mail: prc5@case.edu.

Funding

This work was supported by National Institute of Health (NIH) GM54072 to P.R.C. and R01AI104841 to A.C.A and D.L.W.

Notes

The authors declare no competing financial interest.

■ ACKNOWLEDGMENTS

We are grateful to Stephanie Reeve for providing *S. aureus* DHFR crystal.

■ ABBREVIATIONS

DHFR, Dihydrofolate reductase; IPTG, Isopropyl β-D-1-thiogalactopyranoside; DMSO, Dimethyl sulfoxide; OD, Optical density

■ REFERENCES

(1) Lewis, K. (2013) Platforms for antibiotic discovery. *Nat. Rev. Drug Discovery 12*, 371–387.

(2) Kascakova, S., Maigre, L., Chevalier, J., Refregiers, M., and Pages, J. M. (2012) Antibiotic transport in resistant bacteria: synchrotron UV fluorescence microscopy to determine antibiotic accumulation with single cell resolution. *PLoS One 7*, e38624.

(3) Zimmermann, W. (1980) Penetration of beta-lactam antibiotics into their target enzymes in pseudomonas-aeruginosa - comparison of a highly sensitive mutant with its parent strain. *Antimicrob. Agents Chemother. 18*, 94–100.

(4) Farmer, T. H., Degnan, B. A., and Payne, D. J. (1999) Penetration of beta-lactamase inhibitors into the periplasm of Gram-negative bacteria. *FEMS Microbiol. Lett. 176*, 11–15.

(5) Lakaye, B., Dubus, A., Joris, B., and Frere, J. M. (2002) Method for estimation of low outer membrane permeability to beta-lactam antibiotics. *Antimicrob. Agents Chemother. 46*, 2901–2907.

(6) Yoshimura, F., and Nikaido, H. (1985) Diffusion of beta-lactam antibiotics through the porin channels of Escherichia coli K-12. *Antimicrob. Agents Chemother. 27*, 84–92.

(7) Carey, P. R. (2006) Spectroscopic characterization of distortion in enzyme complexes. *Chem. Rev. 106*, 3043–3054.

(8) Carey, P. R. (1999) Raman spectroscopy, the sleeping giant in structural biology, awakes. *J. Biol. Chem. 274*, 26625–26628.

(9) Smith, E., and Dent, G. (2005) *Modern Raman spectroscopy: a practical approach*, John Wiley and Sons, West Sussex, U.K.

(10) Carey, P. R. (1982) *Biochemical applications of Raman and resonance Raman spectroscopies*, Academic Press, New York.

(11) Huang, W. E., Li, M. Q., Jarvis, R. M., Goodacre, R., and Banwart, S. A. (2010) Shining light on the microbial world: the application of raman microspectroscopy. *Adv. Appl. Microbiol. 70*, 153–186.

(12) Jarvis, R. M., and Goodacre, R. (2008) Characterisation and identification of bacteria using SERS. *Chem. Soc. Rev. 37*, 931–936.

DOI: 10.1021/acs.biochem.5b00202
Biochemistry 2015, 54, 2719–2726

(13) Fu, D., Yu, Y., Folick, A., Currie, E., Farese, R. V., Jr., Tsai, T. H., Xie, X. S., and Wang, M. C. (2014) In vivo metabolic fingerprinting of neutral lipids with hyperspectral stimulated Raman scattering microscopy. *J. Am. Chem. Soc. 136*, 8820−8828.
(14) Zhang, X., Roeffaers, M. B., Basu, S., Daniele, J. R., Fu, D., Freudiger, C. W., Holtom, G. R., and Xie, X. S. (2012) Label-free live-cell imaging of nucleic acids using stimulated Raman scattering microscopy. *ChemPhysChem 13*, 1054−1059.
(15) Fu, D., Zhou, J., Zhu, W. S., Manley, P. W., Wang, Y. K., Hood, T., Wylie, A., and Xie, X. S. (2014) Imaging the intracellular distribution of tyrosine kinase inhibitors in living cells with quantitative hyperspectral stimulated Raman scattering. *Nat. Chem. 6*, 614−622.
(16) Salehi, H., Derely, L., Vegh, A. G., Durand, J. C., Gergely, C., Larroque, C., Fauroux, M. A., and Cuisinier, F. J. G. (2013) Label-free detection of anticancer drug paclitaxel in living cells by confocal Raman microscopy, *Appl. Phys. Lett. 102*.
(17) Ling, J., Weitman, S. D., Miller, M. A., Moore, R. V., and Bovik, A. C. (2002) Direct Raman imaging techniques for study of the subcellular distribution of a drug. *Appl. Opt. 41*, 6006−6017.
(18) Baik, J., and Rosania, G. R. (2011) Molecular imaging of intracellular drug-membrane aggregate formation. *Mol. Pharmaceutics 8*, 1742−1749.
(19) Carey, P. R. (2006) Raman crystallography and other biochemical applications of Raman microscopy. *Annu. Rev. Phys. Chem. 57*, 527−554.
(20) Carey, P. R., Chen, Y. Y., Gong, B., and Kalp, M. (2011) Kinetic crystallography by Raman microscopy. *Biochim. Biophys. Acta, Proteins Proteomics 1814*, 742−749.
(21) Torkabadi, H. H., Bethel, C. R., Papp-Wallace, K. M., de Boer, P. A. J., Bonomo, R. A., and Carey, P. R. (2014) Following drug uptake and reactions inside escherichia coil cells by raman microspectroscopy. *Biochemistry 53*, 4113−4121.
(22) Baba, T., Ara, T., Hasegawa, M., Takai, Y., Okumura, Y., Baba, M., Datsenko, K. A., Tomita, M., Wanner, B. L., and Mori, H. (2006) Construction of Escherichia coli K-12 in-frame, single-gene knockout mutants: the Keio collection, *Mol. Syst. Biol. 2*.
(23) Frey, K. M., Liu, J., Lombardo, M. N., Bolstad, D. B., Wright, D. L., and Anderson, A. C. (2009) Crystal structures of wild-type and mutant methicillin-resistant Staphylococcus aureus dihydrofolate reductase reveal an alternate conformation of NADPH that may be linked to trimethoprim resistance. *J. Mol. Biol. 387*, 1298−1308.
(24) Stephens, P. J., Devlin, F. J., Chabalowski, C. F., and Frisch, M. J. (1994) Ab-initio calculation of vibrational absorption and circular-dichroism spectra using density-functional force-fields. *J. Phys. Chem. 98*, 11623−11627.
(25) Kim, K., and Jordan, K. D. (1994) Comparison of density-functional and MP2 calculations on the water monomer and dimer. *J. Phys. Chem. 98*, 10089−10094.
(26) Leopold, N., Cinta-Pinzaru, S., Baia, M., Antonescu, E., Cozar, O., Kiefer, W., and Popp, J. (2005) Raman and surface-enhanced Raman study of thiamine at different pH values. *Vibr. Spectrosc. 39*, 169−176.
(27) Wunder, S. L., Bell, M. I., and Zerbi, G. (1986) Band broadening of CH_2 vibrations in the Raman-spectra of polymethylene chains. *J. Chem. Phys. 85*, 3827−3839.
(28) Liu, J. Y., Bolstad, D. B., Smith, A. E., Priestley, N. D., Wright, D. L., and Anderson, A. C. (2008) Structure-guided development of efficacious antifungal agents targeting Candida glabrata dihydrofolate reductase. *Chem. Biol. 15*, 990−996.
(29) Vandecasteele, S. J., Peetermans, W. E., Merckx, R., and Van Eldere, J. (2001) Quantification of expression of Staphylococcus epidermidis housekeeping genes with Taqman quantitative PCR during in vitro growth and under different conditions. *J. Bacteriol. 183*, 7094−7101.
(30) Kiefer, W., and Bernstei, Hj. (1971) Rotating Raman sample technique for colored crystal powders - resonance Raman effect in solid $KMn0_4$. *Appl. Spectrosc. 25*, 609−613.

DOI: 10.1021/acs.biochem.5b00202
Biochemistry 2015, 54, 2719−2726